A comparison of ICA-based artifact reduction methods for MEG

A. Ziehe[1], G. Nolte[2], T. Sander[2], K.-R.Müller[1,3] and G. Curio[2]

[1] *GMD FIRST.IDA, Kekuléstr. 7, 12489 Berlin, Germany*
[2] *Neurophysics Group, UKBF, Free University Berlin, Hindenburgdamm 30, 12200 Berlin, Germany*
[3] *University of Potsdam, Am Neuen Palais 10, 14469 Potsdam, Germany*

1 Introduction

In the analysis of MEG data one often faces the problem that noise from biological or technical origins (e.g. alpha activity or interference from the power line, respectively) is corrupting the measurements. We present a case study where we analyze the effects of artifact removal for a well-known experimental setting: measurements of somatosensory evoked fields (SEF, N20). We compare a classical signal processing approach to the recently developed independent component analysis (ICA) technology [9, 11]. The specific data set studied is an attractive testbed since the signal of interest (N20) is relatively strong, but contaminated by a 150 Hz component due to power line interference.

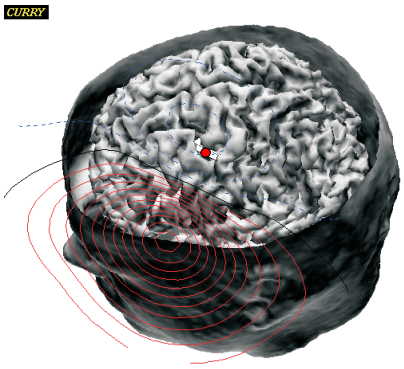

Figure 2: *SEF: Localization of an ECD at the time instance of N20 using a realistic volume conductor model.*

2 Methods

2.1 Data

The right median nerve was stimulated electrically over 12000 epochs, while the magnetic field above the contralateral somatosensory cortex was measured by the Berlin 49 channel planar gradiometer system placed in a magnetically shielded room. A sampling rate of 2 kHz and an inter-stimulus interval (ISI) of 333 msec (to avoid steady state effects) were used (see Fig. 1 and 2).

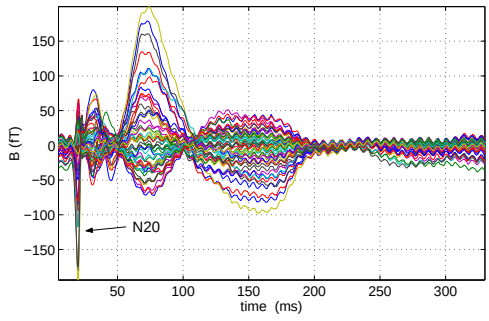

Figure 1: *SEF: averaged time courses of the magnetic field for all 49 channels.*

2.2 ICA model

Due to the fact that magnetic fields of different bioelectric current sources superimpose linearly, the measured values of the SQUID-sensor array can be modeled as a linear combination of component vectors

$$\mathbf{x}(t) = \mathbf{A}\mathbf{s}(t), \tag{1}$$

where $\mathbf{x} = [x_1, \ldots, x_m]^T$, $\mathbf{s} = [s_1, \ldots, s_n]^T$, $m \geq n$. For independent component analysis we assume that the observed signals $\mathbf{x}(t)$ are linear mixtures of n underlying sources $\mathbf{s}(t)$, that are mutually statistically independent, i.e. their joint probability density function factorizes.
Within these assumptions one can separate the data $\mathbf{x}(t)$ into *independent* components $\mathbf{u}(t) = \mathbf{W}\mathbf{x}(t)$. This recovers the original sources $\mathbf{s}(t)$ from the observed mixtures up to scaling and permutation. As both the mixing process $\mathbf{A}$ and the sources $\mathbf{s}(t)$ are unknown, this technique is called *blind source separation* [3].

2.3 Three Algorithms

In the following we will briefly review three representative types of source separation algorithms that take different approaches to achieve a demixing.

A substantial amount of research has been conducted on algorithms using higher-order statistics for estimation of ICA [3]. For off-line (batch) computation, Cardoso et al. [2] developed the **JADE** algorithm based on the (joint) diagonalization of matrices obtained from 'parallel slices' of the fourth-order cumulant tensor. Maximizing the kurtosis of the output signals was also proposed by Hyvärinen and Oja [4]. They developed an algorithm termed **FastICA** that utilizes a fixed-point iteration to optimize a contrast function that measures the distance of the source probability distributions from a Gaussian distribution [3, 4].

In matrix notation FastICA takes the form

$$\mathbf{W}' = \mathbf{W} + \Gamma[\mathrm{diag}(-\beta_i) + E\{g(\mathbf{u})\mathbf{u}^T\}]\mathbf{W},$$

where $\mathbf{u} = \mathbf{W}\mathbf{x}$, $\beta_i = E\{u_i g(u_i)\}$ and $\Gamma = \mathrm{diag}(1/(\beta_i - E\{g'(u_i)\}))$ where $g(u_i)$ is a non-linear contrast function. If one would use $g(u_i) = u_i^3$ the Kurtosis is optimized (as in JADE). Therefore we chose the hyperbolic tangent and the Gaussian function as non-linearities $g(\cdot)$ in our experiments with FastICA.

The two methods mentioned above utilize higher-order statistics to exploit the non-Gaussian distribution of the sources to achieve a separation. In contrast the **TDSEP** (Temporal Decorrelation SEParation) algorithm [10, 11] relies on distinctive spectral/temporal characteristics of the sources using only second-order statistics in the form of (time-delayed) correlation matrices (see also [6, 1]).

The TDSEP algorithm makes use of the property that the cross-correlation functions of mutually independent signals are approximately zero. Assuming further that the signals $\mathbf{s}(t)$ have a temporal structure i.e. a 'non-delta' auto-correlation function all time-delayed correlation matrices $R_{\tau(\mathbf{s})}$ should be non-zero diagonal matrices. This knowledge is used to calculate the unknown mixing matrix $\mathbf{A}$ in eq. (1) by a simultaneous diagonalization of a *set* of correlation matrices[1] $R_{\tau(\mathbf{x})} = \langle \mathbf{x}(t)\mathbf{x}^T(t-\tau)\rangle$ for different choices of τ. Since the mixing model in eq. (1) is simply a linear transformation, we can substitute $\mathbf{x}(t)$ by $\mathbf{A}\mathbf{s}(t)$ and get:

$$R_{\tau(\mathbf{x})} = \langle \mathbf{A}\mathbf{s}(t)\ (\mathbf{A}\mathbf{s}(t-\tau))^T\rangle = \mathbf{A}R_{\tau(\mathbf{s})}\mathbf{A}^T. \quad (2)$$

[1] here $\langle\cdot\rangle$ denotes the time average

For the special case of *two* lagged correlation matrices, e.g. $\tau = 0$ and $\tau \neq 0$ one can achieve a joint diagonalization by solving the general eigenvalue problem $(R_{\tau\neq 0(\mathbf{x})}R^{-1}_{\tau=0(\mathbf{x})})\mathbf{A} = \mathbf{A}\Lambda$ [6].

The quality of the signal separation depends on the choice of τ [10] because for some τ the eigenvalue problem can be degenerated. However, solving eq. (2) for several[2] τ by simultaneous diagonalization eliminates this problem. An approximate simultaneous diagonalization of several matrices can be performed in two steps: (1) sphering and (2) a number of Jacobi rotations (orthogonal transformation). First, the sphering operation $\mathcal{W} = R_{\tau=0}(\mathbf{x})^{-\frac{1}{2}}$ transforms the covariance matrix of $\mathbf{z}(t) = \mathcal{W}\mathbf{x}(t)$ into the identity matrix. Then the remaining set of time-delayed correlation matrices $R_{\tau(\mathbf{z})}$ can be diagonalized subsequently by a unique orthogonal transformation $\mathbf{Q}$, since in the new basis $\mathbf{z}$ all degrees of freedom left are rotations. For details we refer to [2, 1].

Concatenation of both transforms finally yields an estimate of the mixing matrix $\mathbf{A} = \mathcal{W}^{-1}\mathbf{Q}$, which has to be inverted to get the demixing matrix $\mathbf{W} = \mathbf{A}^{-1}$.

2.4 Artifact reduction using ICA

ICA has been a sucessful technique for artifact reduction in EEG and MEG [5, 9, 11]. Our ICA-based artifact reduction procedure consist of the following steps: First, a sphering and compression by PCA is applied. For our data we reduced the 49 input dimensions to 15 based on the Eigenvalue spectrum shown in Fig. 3a. Then we decompose the transformed data into independent components by an ICA algorithm. In a next step we decide which components correspond to artifactual or relevant signals on the basis of prior knowledge. Finally we project the previously selected components of interest back to sensor space and by doing so we obtain a set of cleaned measurements.

Another option is to remove the artifact fields by making use of their estimated spatial structure (contained in the columns of the mixing matrix $\mathbf{A}$) by Signal-Space Projection (SSP) [7, 8]. In case of multiple artifacts the whole space spanned by these artifacts, which we will refer to as 'artifact space', has to be projected out. The essential requirement for applying SSP is that the unwanted fields are to be known (up to multiplicative constants) which is fulfilled if the ICA merely finds the artifact space correctly.

[2] In the experiments we chose $\tau = 0..5$.

2.5 Performance Evaluation

We make use of the fact that the ISI is relatively large and fit the parameters of a notch filter on the last part (> 200ms) of the averaged data (see Fig. 1) and extrapolate this to the first part. This corrected data is refered to as "gold standard". To assess the performance of the different artifact reduction methods, the normalized deviation from the "gold standard" is used. As a second criteria of interest we compare the goodness-of-fit of an equivalent current dipole (ECD) model for a realistic volume conductor (calculations were performed with the CURRY software package).

3 Results

Predominantly two artifactual 150 Hz components (Fig. 4) were identified by the ICA decomposition in a fully automatic, data-driven manner. Fig. 3b clearly shows that the energy present in almost all 49 channels in the 150Hz band in the original data (top graph) is condensed to fewer ones using PCA (lower left). Finally in the ICA basis only two 150 Hz components persist (lower right). Fig. 5 reveals that ICA techniques eliminating these artifact fields yield similar results – only 2-3% deviation – as the "gold standard" notch filtering approach, provided that the sample size is sufficiently large i.e. > 400 (see Fig. 5). Note that a crude (non-adaptive) notch filter yields a constant error of approximately 8%, which is much worse than for the ICA based algorithms. To obtain Fig. 6, we project the data orthogonal to the artifact subspace and give the deviation from the accordingly projected gold standard data, which yields remarkably better results, especially for small sample sizes. Here we can obtain an improvement in deviation of a factor 10 compared to the simple subtraction approach shown in Fig. 5.

The goodness-of-fit of the dipole model is very high for all methods (even for the original data), due to the high signal to noise ratio at N20. Interestingly, if ICA is used, one achieves accuracies of larger than 99.8%.

4 Discussion

In our testbed scenario, we have access to the "ground truth" since we know that mainly a 150Hz distortion is present, and due to the large inter-stimulus interval we are able to adapt parameters of a notch filter effectively. In the general setting where no such a priori information is available, it is apparent that such

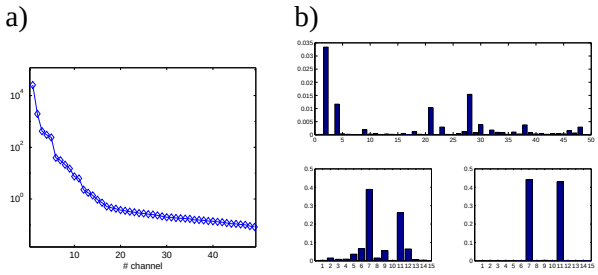

Figure 3: *a) Eigenvalue spectrum of the covariance matrix of the data. b) relative power in the 150 Hz band for original data, PCA and ICA, respectively.*

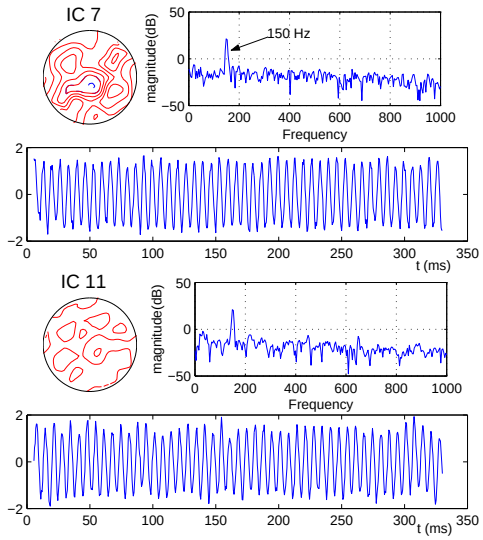

Figure 4: *Two components showing a strong peak at 150 Hz were obtained by ICA (here the TDSEP algorithm was applied to a 15-dimensional subspace of the data).*

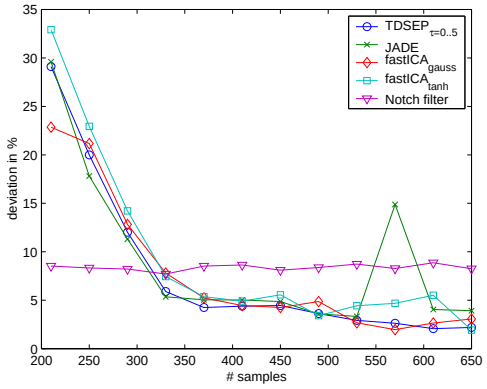

Figure 5: *Deviation from the gold standard for different artifact removal methods using subtraction.*

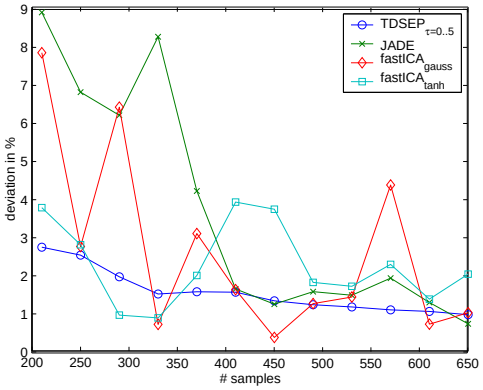

Figure 6: *Deviation from the gold standard for ICA-based methods using projection.*

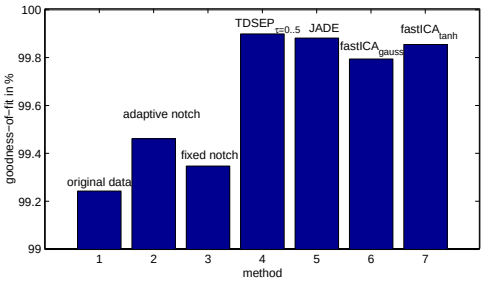

Figure 7: *Goodness-of-fit for an ECD using different methods.*

notch filtering would inevitably fail while ICA can still yield reasonable results. Furthermore, the combination of ICA with SSP to eliminate artifacts has proven superior to methods that merely subtract the noise. Our artifact reduction methods are fully automated, and they could be applied to any multichannel data, provided that there exist criteria to spot the artifacts.

Finally, for the ICA-based methods, e.g. for TDSEP (cf. Fig. 6), shorter inter-stimulus intervals would be possible without losses in localization accuracy.

Future research will furthermore focus on strategies for combining projection techniques and ICA incorporating a-priori knowledge.

Acknowledgements A.Z. and K.R.M. acknowledge partly funding by the EC Project #IST-1999-14190-BLISS. G.N., T.S. and G.C. were supported by DFG grant MA 1782/3-1. We also thank the Biomagnetism group of PTB for providing the measurement facilities and valuable discussions.

References

[1] A. Belouchrani, K. Abed Meraim, J.-F. Cardoso, and E. Moulines. A blind source separation technique based on second order statistics. *IEEE Trans. on SP*, 45(2):434–44, Feb 1997.

[2] J.-F. Cardoso and A. Souloumiac. Blind beamforming for non Gaussian signals. *IEE Proceedings-F*, 140(6):362–370, 1993.

[3] P. Comon. Independent component analysis, a new concept? *Signal Processing, Elsevier*, 36(3):287–314, 1994.

[4] A. Hyvärinen and E. Oja. A fast fixed-point algorithm for independent component analysis. *Neural Computation*, 9(7):1483–1492, 1997.

[5] S. Makeig, T-P. Jung, D. Ghahremani, A.J. Bell, and T.J. Sejnowski. Blind separation of event-related brain responses into independent components. *Proc. Natl. Acad. Sci. USA*, 94:10979–10984, 1997.

[6] L. Molgedey and H.G. Schuster. Separation of a mixture of independent signals using time delayed correlations. *Physical Review Letters*, 72(23):3634–3637, 1994.

[7] G. Nolte and G. Curio. The effect of artifact rejection by signal-space projection on source localization accuracy in MEG measurements. *IEEE Trans. Biomed. Eng.*, 46:400–408, 1999.

[8] M.A. Uusitalo and R.J. Ilmoniemi. The signal-space projection (SSP) method for separating MEG or EEG into components. *Med.Biol.Eng.Comput.*, 35:135–140, 1997.

[9] R. Vigário, V. Jousmäki, M. Hämäläinen, R. Hari, and E. Oja. Independent component analysis for identification of artifacts in magnetoencephalographic recordings. In Jordan, Kearns, and Solla, editors, *Proc. NIPS 10*. The MIT Press, 1998.

[10] A. Ziehe and K.-R. Müller. TDSEP – an efficient algorithm for blind separation using time structure. In Niklasson, Bodén, and Ziemke, editors, *Proc. ICANN'98*, pages 675 – 680, Skövde, 1998.

[11] A. Ziehe, K.-R. Müller, G. Nolte, B.-M. Mackert, and G. Curio. Artifact reduction in magnetoneurography based on time-delayed second order correlations. *IEEE Trans. Biomed. Eng.*, 47(1):75–87, 2000.